第 33 卷第 10 期　　焊　接　学　报　　Vol. 33　No. 10
2012 年 10 月　　TRANSACTIONS OF THE CHINA WELDING INSTITUTION　　October　2012

水下湿法药芯焊丝焊接电弧稳定性

石永华，　郑泽培，　黄　晋
（华南理工大学 机械与汽车工程学院，广州　510640）

石永华

摘　要： 利用焊接电弧电压信号的标准差和差异系数的倒数作为评价电弧稳定性的指标，通过试验研究了不同工艺条件下水下湿法药芯焊丝焊接的电弧稳定性. 建立了湿法焊接电弧稳定性的敏感度模型，分析了各工艺参数如焊接电流、电弧电压、焊接速度和水深对湿法药芯焊丝焊接电弧稳定性的影响. 结果表明，水深增大时，焊接电弧稳定性变差，特别是在浅水区域，增大水深可显著降低电弧稳定性；焊接速度增大，电弧稳定性变差；焊接电压对电弧稳定性影响很大，适当提高焊接电压可提高电弧的稳定性.

关键词： 水下焊接；　电弧稳定性；　敏感度分析
中图分类号： TG403　　**文献标识码：** A　　**文章编号：** 0253－360X(2012)10－0049－05

0　序　　言

随着海洋资源开发力度的日益加大，海洋工程结构物也日益增多. 水下湿法焊接施工方便灵活，在海底管线、石油平台和码头、大桥等的施工和维修中的应用日益广泛. 稳定的电弧是获得良好的弧焊质量的基础. 由于受到水和压力的影响，水下焊接电弧需要更高的电场强度才能将弧柱区的气体电离及保持电弧的持续燃烧. 水下焊接工艺参数和水压对水下焊接电弧的稳定性有很大的影响. 随着水深增加，维持焊接过程稳定的焊接工艺参数范围都显著变窄[1]. 国内外学者对高压干法水下焊接和空气中焊接的电弧稳定性进行了研究[2-5]；文献[6]对浅水下湿法焊条电弧焊的电弧稳定性进行了研究，但对于水下湿法药芯焊丝焊接（FCAW，flux cored arc welding）的电弧稳定性目前尚无相关的研究报道.

为了研究影响水下湿法 FCAW 电弧稳定性的关键因素，文中对水下湿法 FCAW 的电信号进行了分析，以电弧电压变异系数的倒数作为电弧稳定性的指标，并基于敏感度分析的方法量化分析了焊接工艺参数对水下湿法 FCAW 电弧稳定性的影响程度的大小，研究结果可为提高水下焊接质量提供理论基础.

收稿日期： 2012－01－09
基金项目： 国家自然科学基金资助项目（51175185，50705030）；中央高校基本科研业务费专项资金资助项目（2012ZZ0052）；广东省自然科学基金资助项目（9151064101000065）

1　试验设备及材料

水下湿法 FCAW 试验在压力舱内进行，如图 1 所示. 水下焊接前向压力舱内注入水，使焊接时电弧处于水中，向舱内注入不同压力的压缩气体来模拟不同的水深. 水下焊接采用直径 2.0 mm 的自保护药芯焊丝，在 Q235 钢板表面进行堆焊.

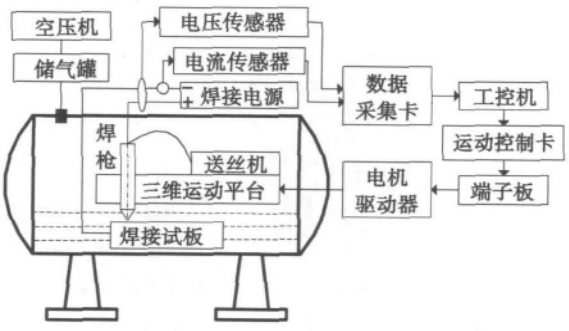

图 1　压力舱水下湿法 FCAW 及数据采集系统

Fig. 1　Hyperbaric underwater wet FCAW and welding electrical data acquisition system

2　水下焊接电信号波形

在焊接材料确定的情况下，影响水下焊接质量的因素主要有：焊接电流、电弧电压、导电嘴至工件距离 l_{CTWD}、焊接速度和水深（压力）. 当焊接速度为 10 mm/s，电弧电压为 31 V，l_{CTWD} 为 20 mm 时采集的水下焊接电流和电压信号如图 2 所示. 可见水下湿

法 FCAW 的电流和电压波动比较剧烈.

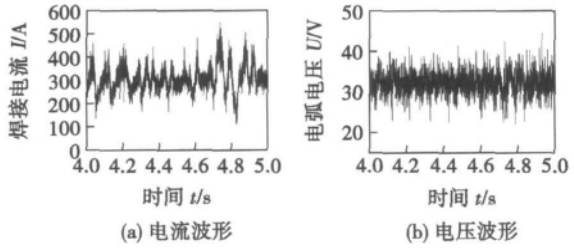

图 2 水下湿法 FCAW 的电流和电压波形

Fig. 2 Arc current and voltage waveform of underwater wet FCAW

3 水下焊接电信号稳定性指标

焊接电弧电压 U 一般与弧长成正比,因此当电弧不稳定时必然导致电弧电压和焊接电流 I 的波动. 反过来,电弧电压和焊接电流的波动性也反映了电弧的稳定性. 从统计学的角度,焊接电流极差ΔI 和焊接电压极差ΔU、电压标准差 U_σ 和电流标准差 I_σ、电压差异系数($C_U = U_\sigma / U$) 和电流差异系数($C_I = I_\sigma / I$) 可成为衡量电压或电流稳定性的三个指标[3]. 极差、标准差和差异系数越小,则电信号波动性越小,表示电压或电流越稳定. 由于信号的极差容易受偶然因素的影响,文中利用标准差和差异系数来衡量电弧稳定性. 又由于差异系数计算值很小,因此用其倒数(C_U^{-1},C_I^{-1}) 来表示.

在高压舱内进行湿法 FCAW 试验,通过霍尔传感器采集焊接电流和电压,将其输入数据采集卡,开发 Labview 数据采集和处理软件来采集焊接电信号,并统计不同焊接条件下的 U_σ,I_σ,C_U^{-1} 和 C_I^{-1}.

当 l_{CTWD}为 20 mm,焊接速度为 10 mm/s,电弧电压为 34 V,水深为 0.2 m 时,电弧稳定性指标与电流的关系如图 3 所示. 可见,随着电流增大,电流标准差呈增大的趋势,说明电弧稳定性有所降低,但降低的幅度不大.

当焊接电流为 320 A,焊接速度为 10 mm/s,焊接水深为 0.2 m 时,电流标准差和差异系数的倒数与电弧电压的关系如图 4 所示. 可见,当电弧电压小于 32 V 时,焊接电弧稳定性随电压增大而增大,32 V 时电弧最稳定,而当电弧电压超过 32 V 时,电弧稳定性显著下降.

当焊接电流为 310 A,焊接速度为 10 mm/s,电弧电压为 30 V 时,电弧电压标准差、相对标准差的倒数与焊接水深的关系如图 5 所示. 显然,随着水深的增加,电弧稳定性明显下降.

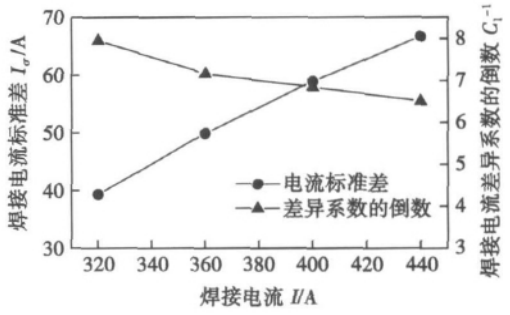

图 3 标准差和差异系数与电流的关系

Fig. 3 Influence of welding current on current standard deviation and relative standard deviation

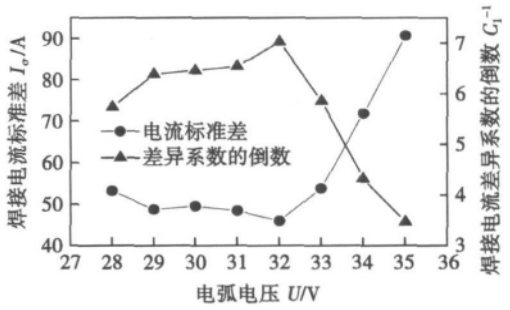

图 4 焊接电流标准差和变异系数与电弧电压的关系

Fig. 4 Influence of welding voltage on current standard deviation and relative standard deviation

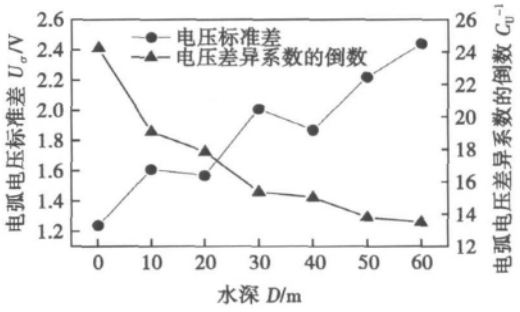

图 5 电弧电压标准差和差异系数与水深的关系

Fig. 5 Influence of welding current on standard deviation and relative standard deviation of welding voltage

4 电弧稳定性因素的敏感度分析

4.1 经验公式的建立

大量试验结果证实,一般焊接稳定性随焊接工艺参数(电流、电压等) 的变化是单调的类似于指数曲线的关系,因此可用以下的经验公式表示,即

$$U_\sigma = a_0 I^{a_1} U^{a_2} v^{a_3} D^{a_4} \quad (1)$$

$$C_U^{-1} = a'_0 I^{a'_1} U^{a'_2} v^{a'_3} D^{a'_4} \quad (2)$$

式中: v 为焊接速度; D 为焊接水深; a_0 和 a'_0 为常

数; a_1,a_2,a_3,a_4 以及 a'_1,a'_2,a'_3,a'_4 为回归系数.

把式(1),式(2)两端分别取对数可得

$$\ln U_\sigma = \ln a_0 + a_1 \ln I + a_2 \ln U + a_3 \ln v + a_4 \ln D \quad (3)$$

$$\ln(C_U^{-1}) = \ln a'_0 + a'_1 \ln I + a'_2 \ln U + a'_3 \ln v + a'_4 \ln D \quad (4)$$

选择焊接电流、电弧电压、焊接速度和水深作为影响水下焊接电弧稳定性的主要因素,l_{CTWD} 固定为 20 mm,在焊接压力舱内进行了 25 次试验,分别采集焊接电压信号并计算焊接电压标准差和电压差异系数的倒数. 焊接参数及结果如表 1 所示.

表 1　水下焊接电弧稳定性试验参数及结果

Table 1　Experimental parameters and results of underwater welding arc stability

电流 I/A	电压 U/V	焊接速度 v/(mm/s)	水深 D/m	电压标准差 U_σ/V	电压差异系数的倒数 C_U^{-1}
320	34	10	0.1	1.07	32.31
340	34	10	0.1	1.23	27.63
360	34	10	0.1	1.33	25.53
380	34	10	0.1	1.41	23.97
400	34	10	0.1	1.36	23.06
420	34	10	0.1	1.40	22.23
440	34	10	0.1	1.54	22.13
460	34	10	0.1	1.57	21.72
320	30	10	0.1	1.36	21.98
320	31	10	0.1	1.20	26.06
320	32	10	0.1	1.15	27.80
320	33	10	0.1	1.02	32.21
320	34	10	0.1	1.07	32.31
320	35	10	0.1	1.04	33.93
300	32	6	0.1	1.13	28.37
300	32	8	0.1	1.14	27.92
300	32	10	0.1	1.23	26.13
300	32	12	0.1	1.15	25.23
310	30	10	0.1	1.24	24.25
310	30	10	10	1.61	19.08
310	30	10	20	1.57	17.85
310	30	10	30	2.01	15.38
310	30	10	40	1.87	15.04
310	30	10	50	2.22	13.80
310	30	10	60	2.44	13.50

根据表 1 所示的焊接电压标准差和差异系数的倒数,可以利用多元线形回归方法确定式(3),式(4)的回归系数,可得

$$U_\sigma = 0.323 I^{1.0043} U^{-1.2358} v^{-0.0104} D^{0.0780} \quad (5)$$

$$C_U^{-1} = 3.713 I^{-1.0688} U^{2.3297} v^{-0.0485} D^{-0.0737} \quad (6)$$

根据式(5),式(6)计算出的电弧电压标准差和差异系数的倒数与实际测量值的比较如图 6 所示. 可见,该模型的计算值是比较准确的.

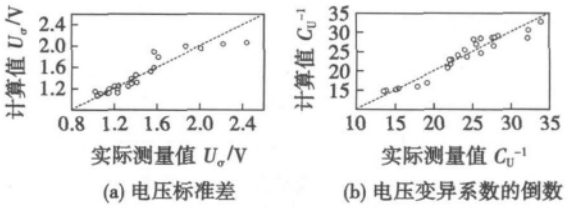

图 6　U_σ 和 C_U^{-1} 的理论计算值与实际测量值的比较

Fig. 6　Calculated and measured U_σ and C_U^{-1} in arc stability analysis

4.2　水下焊接稳定性的敏感度分析

敏感度分析是一种辨别关键影响因素并将其按重要性进行排序的数学方法[7,8]. 文中利用其来量化分析各焊接工艺参数对电弧稳定性的影响程度,并确定影响电弧稳定性的最主要工艺参数.

将式(5),(6)分别对焊接工艺参数 I,U,v,D 求导数,可获得相应的敏感度公式,即

$$\mathrm{d}(U_\sigma)/\mathrm{d}I = 0.324 I^{0.0043} U^{-1.2358} v^{-0.0104} D^{0.0780} \quad (7)$$

$$\mathrm{d}(C_U^{-1})/\mathrm{d}I = -3.968 I^{-2.0688} U^{2.3297} v^{-0.0485} D^{-0.0737} \quad (8)$$

电弧电压的敏感度公式为

$$\mathrm{d}(U_\sigma)/\mathrm{d}U = -0.399 I^{1.0043} U^{-2.2358} v^{-0.0104} D^{0.0780} \quad (9)$$

$$\mathrm{d}(C_U^{-1})/\mathrm{d}U = 8.65 I^{-1.0688} U^{1.3297} v^{-0.0485} D^{-0.0737} \quad (10)$$

焊接速度的敏感度公式为

$$\mathrm{d}(U_\sigma)/\mathrm{d}v = -0.0034 I^{1.0043} U^{-1.2358} v^{-1.0104} D^{0.0780} \quad (11)$$

$$\mathrm{d}(C_U^{-1})/\mathrm{d}v = -0.18 I^{-1.0688} U^{2.3297} v^{-1.0485} D^{-0.0737} \quad (12)$$

焊接水深的敏感度公式为

$$\mathrm{d}(U_\sigma)/\mathrm{d}D = 0.0238 I^{1.0043} U^{-1.2358} v^{-0.0104} D^{-0.922} \quad (13)$$

$$\mathrm{d}(C_U^{-1})/\mathrm{d}D = -0.274 I^{-1.0688} U^{2.3297} v^{-0.0485} D^{-1.0737} \quad (14)$$

当 v = 10 mm/s,浅水 0.1 m 焊接时,敏感度数据如表 2 所示. 电弧电压对稳定性指标的敏感度是正的,而焊接电流、焊接速度和焊接水深对电弧稳定性指标(差异系数的倒数)的敏感度是负的.

敏感度为正值表示当电弧电压增大时,差异系数的倒数也增大,从而电弧稳定性也增大. 敏感度为负值表示当焊接电流、焊接速度和焊接水深增大

表 2 电弧稳定性敏感度分析

Table 2 Sensitivity analysis of arc stability

焊接电流 I/A	电弧电压 U/V	计算值 C_U^{-1}	电流敏感度 $\mathrm{d}(C_U^{-1})/\mathrm{d}I$	电压敏感度 $\mathrm{d}(C_U^{-1})/\mathrm{d}U$	焊接速度敏感度 $\mathrm{d}(C_U^{-1})/\mathrm{d}v$	水深敏感度 $\mathrm{d}(C_U^{-1})/\mathrm{d}D$
320	28	19.45	−0.064 9	1.618 1	−0.094 3	−14.351 3
370	28	16.65	−0.048 1	1.385 5	−0.080 7	−12.288 5
420	28	14.54	−0.037 0	1.210 0	−0.070 5	−10.731 6
320	32	26.54	−0.088 6	1.932 5	−0.128 7	−19.588 2
370	32	22.73	−0.065 6	1.654 7	−0.110 2	−16.772 8
420	32	19.85	−0.050 5	1.445 1	−0.096 2	−14.647 7
320	36	34.92	−0.116 6	2.260 1	−0.169 3	−25.773 0
370	36	29.90	−0.086 4	1.935 3	−0.145 0	−22.068 6
420	36	26.12	−0.066 5	1.690 1	−0.126 6	−19.272 6

时，差异系数的倒数减小，即电弧稳定性降低. 敏感度的绝对值越大，表示对差异系数倒数的影响程度越大. 因此水深对电弧稳定性恶化的影响程度要大于焊接电流和焊接速度.

图 7 显示了当焊接电压为 32 V 时，总体上焊接电流和焊接速度增大，电弧稳定性降低. 其原因是水下焊接时电弧在气泡中燃烧，焊接速度大，气泡受到水的阻力也大，从而干扰了其中的焊接电弧，导致电弧稳定性降低. 但随焊接电流和焊接速度增大，对电弧稳定性的影响程度变小.

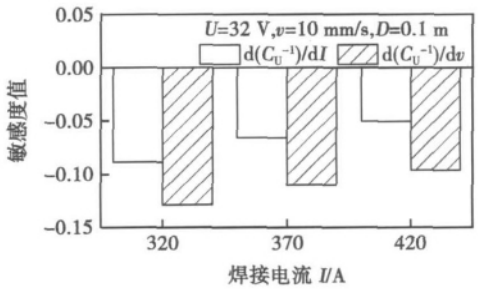

图 7 焊接电流和焊接速度的敏感度分析结果

Fig. 7 Sensitivity analysis results of welding current and welding speed

图 8 显示当焊接电流为 370 A 时，总体上焊接电压增大，电弧稳定性增大，焊接水深增大，电弧稳定性降低，随电弧电压增大，对电弧稳定性的影响程度也变大. 随着水深增大，对电弧稳定性的影响程度也显著增大.

图 9 为焊接水深对电弧稳定性的敏感度分析. 从图 9 可以看出，焊接水深对 C_U^{-1} 的敏感度呈负值，特别是浅水下随着水深增加而电弧稳定性恶化，但在深水时，水深的增加对电弧稳定性的恶化程度减小.

图 10 为水深 30 m，电压 32 V，焊接速度为 10

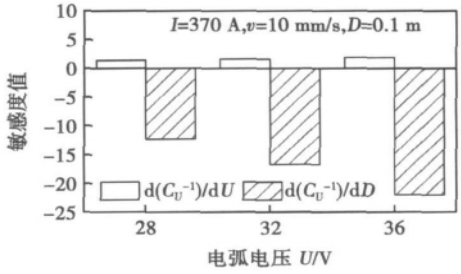

图 8 电弧电压和焊接水深的敏感度分析

Fig. 8 Sensitivity analysis results of welding voltage and water depth

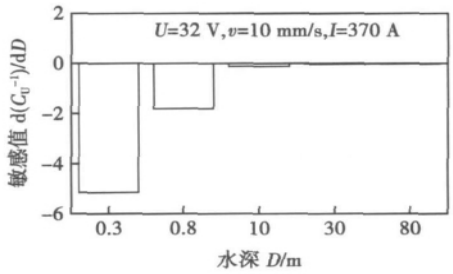

图 9 焊接水深对电弧稳定性的敏感度分析

Fig. 9 Sensitivity of water depth on arc stability

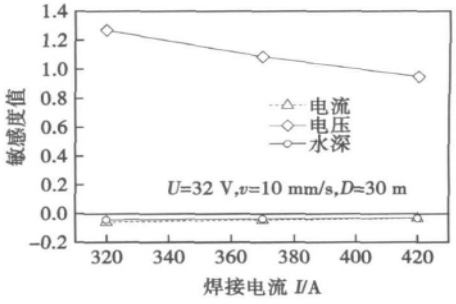

图 10 电压差异系数的倒数的敏感度分析

Fig. 10 Sensitivity analysis of reciprocal of welding voltage relative standard deviation

mm/s 时，电弧稳定性指标与各焊接工艺参数的关系. 电弧电压对电弧稳定性指标的敏感度值是正的，而焊接电流和水深对电弧稳定性指标的敏感度值是负的. 由于电压对电弧稳定性的敏感度值远大于焊接电流和水深，因此在此焊接条件下可通过适当提高电弧电压来稳定电弧.

5　结　　论

(1) 水下焊接时，电弧电压对电弧稳定性有很大影响，适当提高电压可提高电弧的稳定性，但当电压超过最佳电压时，将导致电弧稳定性迅速恶化.

(2) 焊接水深对电弧稳定性的敏感度值为负，表明当水深增大时，焊接电弧稳定性变差. 特别是在浅水区域，增大水深可显著降低电弧稳定性. 而在深水时，水深的增大对电弧稳定性的影响程度变小.

(3) 焊接电流、焊接速度对电弧稳定性的敏感度值为负，在焊接水深和电弧电压一定时增大焊接电流，电弧稳定性变差，但其影响程度较小. 增大焊接速度，也会导致电弧稳定性变差.

(4) 文中的研究结果可促进对水下焊接电弧稳定性机理的理解，也可为湿法水下焊接工艺参数的优化提供理论指导.

参考文献:

[1] Rowe M, Liu S. Recent developments in underwater wet welding [J]. Science and Technology of Welding and Joining, 2001, 6(6): 387 – 396.

[2] Hart P, Richardson I M, Nixon J H. The effects of pressure on electrical Performance and weld bead geometry in high pressure GMA welding [J]. Welding in the World, 2001, 45(11/12): 25 – 33.

[3] 周灿丰，焦向东，薛　龙，等. 高压空气环境钨极氩弧行为和焊接技术的研究 [J]. 船海工程，2008，37(2): 14 – 17.
Zhou Canfeng, Jiao Xiangdong, Xue Long, *et al*. Gas tungsten arc welding behavior features under high air ambient pressure [J]. Ship & Ocean Engineering, 2008, 37(2): 14 – 17.

[4] 焦向东，潘际銮，张　骅. 交流 MAG 焊接电弧稳定性及其控制 [J]. 焊接学报，1998，19(1): 47 – 51.
Jiao Xiangdong, Pan Jiluan, Zhang Hua. A. C. MAG welding arc stabil ity and Its control [J]. Transactions of the China Welding Institution, 1998, 19(1): 47 – 51.

[5] 方臣富，陈树君，刘　嘉，等. SACTIG 与 VPTIG 电弧稳定性的比较分析(一) [J]. 焊接学报，2005，26(12): 1 – 5.
Fang Chenfu, Chen Shujun, Liu Jia, *et al*. Study on arc stability of SACTIG and VPTIG(1). Transactions of the China Welding Institution, 2005, 26(12): 1 – 5.

[6] Mazzaferro J A E, Machado I G. Study of arc stability in underwater shielded metal arc welding at shallow depths [J]. Proceedings of the Institution of Mechanical Engineers, Part C: Journal of Mechanical Engineering Science, 2009, 223(3): 699 – 709.

[7] Kim I S, Son K J, Yang Y S, *et al*. Sensitivity analysis for process parameters in GMA welding processes using a factorial design method [J]. International Journal of Machine Tools & Manufacture, 2003, 43(8): 763 – 769.

[8] Karaoglu S, Secgin A. Sensitivity analysis of submerged arc welding process parameters [J]. Journal of Materials Processing Technology, 2008, 202(1/3): 500 – 507.

作者简介: 石永华，男，1973 年出生，博士，教授. 主要从事水下焊接及自动化的研究工作. 发表论文 30 余篇. Email: yhuashi@scut.eu.cn

fect of HT250 castiron used in diesel engine cylinder was repaired with inferior-laser instantaneous melting cold-welding technology. The cold-welding residual stress was measured through the X-ray diffraction method to study the regularity of residual stress and the relationship between the residual stress and different process parameters. The results show that the stress near the weld seam is tensile and the stress away from the weld seam is compressive. The cold welding residual stress distribution is quite narrow. The peak stress mainly distributes in the range of 5mm from the weld seam center and the residual stress is close to zero in the place of 20 mm away from the weld seam center. Time parameter has little influence on the peak stress while the energy parameter's influence is great. Through the change of time and energy, smaller residual peak stress can be obtained to meet the repair requirements for surface damage on engine remanufacturing parts.

Key words: cold-welding; surface residual stress; process parameters; remanufacturing

Pitting corrosion resistance of PH stainless steel of FV520B and its welding joint ZHANG Min[1], ZHANG Enhua[1], ZHI Jinhua[1,2], MENG Qiang[1], ZHANG Haicun[2] (1. School of Material Science and Engineering, Xi'an University of Technology, Xi'an 710048, China; 2. Xi'an Shangu Power Co., Ltd, Xi'an 710075, China). pp 37 - 40

Abstract: The corrosion-resistance of the steel FV520B had been tested respectively in the HCl and H_2SO_4 (10%) under the 35 ℃. The result showed that under the above condition the base metal and the welding welding joint suffered a much more serious pitting corrosion in the HCl (10%) than that in the H_2SO_4 of the same mass fraction, the chloridion has more serious destructive effect on the passivation film of the stainless steel, which causes the deeper corrosive pitting. while the corrosive effect of 10% mass fraction H_2SO_4 is relatively inferior, the corrosion products are different either, but under the different corrosive environment, all the corrosive level of the weld joint in the welding point is lower than the HAZ.

Key words: precipitation sclerosis stainless steel; microstructure; corrosion resistance

Interfacial microstructure and properties of Si_3N_4 joints brazed using TiNi-V eutectic brazing alloy WANG Guoxing[1], SONG Xiaoguo[2,3], CHEN Haiyan[3], LI Yang[1], CAO Jian[2,3] (1. School of Materials & Chemical Engineering, Heilongjiang Institute of Technology, Harbin 150050, China; 2. School of Materials Science & Engineering, Harbin Institute of Technology at Weihai, Weihai 264209, China; 3. State Key Lab of Advanced Welding and Joining, Harbin Institute of Technology, Harbin 150001, China). pp 41 - 44

Abstract: TiNi-V eutectic brazing alloy was fabricated by vacuum arc melting, and its spreadability on the surface of Si_3N_4 ceramic was investigated. The brazing of Si_3N_4 ceramic was achieved using TiNi-V brazing alloy. The typical interfacial microstructure was Si_3N_4/TiN + Ti-Si compounds/NiV. The effect of brazing temperature on the interfacial microstructure and properties of joints was investigated. The results showed that with the increasing of brazing temperature, the reaction between molten brazing alloy and Si_3N_4 ceramic intensified and the thickness of TiN + Ti-Si compounds layer increased gradually. Moreover, lots of microcracks were formed in the joints due to the residual stress in joints, which deteriorated the joining properties. The highest shear strength of 28 MPa was obtained when the specimen was brazed at 1 200 ℃ for 10 min. The joint fractured in TiN + Ti-Si compounds layer, which belonged to brittle fracture.

Key words: TiNi-V eutectic brazing alloy; brazing; Si_3N_4 ceramic; interfacial microstructure

Fatigue fracture behavior of laser-MIG hybrid welded 7075-T6 aluminium alloys WU Shengchuan[1,2], XU Xiaobo[1], ZHANG Weihua[2], LI Zheng[1], XU Daorong[1] (1. School of Materials Science and Engineering, Hefei University of Technology, Hefei 230009, China; 2. State Key Laboratory of Traction Power, Southwest Jiaotong University, Chengdu 610031, China). pp 45 - 48

Abstract: The influence of stress ratio R and stress range σ_a on the fatigue crack propagation behavior of high strength 7075-T6 aluminum alloy and laser-MIG hybrid welded joint is studied. The results show that under the welding parameters of P = 3 000 W, I = 110A and v = 3 m/min, the fatigue cracking growth rate curve of laser-arc hybrid welding joint intersects with that of base metal. That is due to that the fatigue crack growth rate of hybrid welding joint is lower than that of base metal especially when the SIF range ΔK is less than 15.6 MPa·m$^{1/2}$. Under the conditions of same SIF range ΔK, the fatigue cracking growth rate at the higher stress ratio is larger than that of the lower stress ratio. Furthermore, the stress range is more important than the stress ratio (mean stress) to determine the fatigue cracking growth rate of welding joints.

Key words: hybrid laser-arc welding; 7075 high strength aluminium alloy; fatigue fracture; microstructure; softening effect

Arc stability of underwater wet flux-cored arc welding SHI Yonghua, ZHENG Zepei, HUANG Jin (School of Mechanical and Automotive Engineering, South China University of Technology, Guangzhou 510640, China). pp 49 - 53

Abstract: Standard deviation (SD) and the reciprocal of coefficient of variation (CV) of welding voltage are used as the index of arc stability. The arc stability of underwater wet flux-cored arc welding in different welding conditions was studied based on underwater wet welding experiments. Sensitivity models of arc stability have been built and sensitivities of welding parameters on arc stability, such as welding current, voltage, speed and water depth, were analyzed. The results showed that the arc stability got worse as water depth increased. Especially in shallow water, the arc stability decreased dramatically as the water depth increased. Arc stability also decreases with the increasing of welding speed. The welding voltage has a great influence on arc stability and increasing the welding voltage appropriately will improve the arc stability.

Key words: underwater welding; arc stability; sensitivity analysis